



Interfacial crack front wandering: influence of quenched noise correlations

Jean Schmittbuhl^a, Jean-Pierre Vilotte^{b,*}

^a*Département de Géologie, Unité Mixte de Recherche UMR 8538, École Normale Supérieure, 24 rue Lohmond, 75232 Paris Cedex 05, France*

^b*Département de Sismologie, Unité Mixte de Recherche CNRS UMR 7580 Institut de Physique du Globe de Paris, 4 Place Jussieu, 75252 Paris Cedex 05, France*

Abstract

We discuss the influence of spatially correlated quenched noise on the wandering exponent of the crack-front line during slow in-plane crack propagation. For a uniform noise, the wandering exponent in the stastically stationary regime is $\zeta = 0.35 \pm 0.02$, while the dynamic exponent is $z = 0.75 \pm 0.02$. For short-range Gaussian correlations, the wandering exponent is shown to be $\zeta = 0.50 \pm 0.03$ in the small fluctuation limit and $\zeta = 0.35 \pm 0.02$ in the large fluctuation limit which can be shown to be consistent with the uniform case. In the case of long-range correlations, characterized by a self-affine exponent ζ_t , the wandering exponent is shown to scale as $\zeta = \zeta_t + 1$ for a wide range of ζ_t between -1.0 and $+1.0$. These results are discussed with reference to recent experiments of slow in-plane crack propagation between two annealed Plexiglas blocks. © 1999 Elsevier Science B.V. All rights reserved.

PACS: 62.20.Mk; 61.43.-j; 81.40.Np

Keywords: Interfacial crack; Pinning; Roughness

1. Introduction

Understanding the propagation of rupture front through heterogeneous elastic solids emerges as a key issue for a large number of geophysical and mechanical problems. Even when the rupture front is interfacial, i.e. restricted to move in a plane, the dynamics involves complicated interactions between nonlocal elastic coupling, inertia and wave effects, as well as quenched heterogeneities. In-plane crack front propagation along an heterogeneous interface is observed as non uniform with segments of the

* Corresponding author.

E-mail address: vilotte@ipgp.jussieu.fr (J.-P. Vilotte)

front that are trapped temporarily by local asperities that may be related to local material heterogeneities or residual stresses. The depinning from these asperities involves local instabilities. Even though the exact mechanism of crack/asperity interactions has not yet been clarified, it requires explicit three dimensional modeling due to the fact that long range bulk elastic interactions has to be accounted for the determination of the stress intensity factor variations along the crack front. When the elastic coupling is small, i.e. strong pinning, the dynamics is controlled by individual instabilities. When the elastic coupling is strong, i.e. weak pinning, the dynamics is controlled by the whole front. Moreover when local asperity depinning occurs, dynamical coupling can develop from waves that result in stress overshoots elsewhere on the front.

In recent years, there has been theoretical developments within the context of crack theory. In the framework of first-order perturbation theory a relationship between the stress intensity factor for tensile crack (Mode I) and small deviations from straightness of the edge of a semi-infinite plane crack, extending at constant speed in an infinite elastic body, was first proposed [1,2] using weight functions [3,4] in the approximation of scalar elasticity. This work has been extended to dynamic crack growth both for scalar and vectorial elasticity [5–8] as well as for nonplanar crack growth under mixed loading [9–12].

In an early study [13], it was shown, using a first-order linear perturbation theory for scalar elasticity, that the competition between the elastic energy and the pinning due to the disorder of the interface gives rise, during slow in-plane crack propagation, to a non trivial wandering exponent of the crack front. The stationary state was found to be characterized by an in-plane wandering exponent ζ of the crack front, that is $\zeta \approx 1/3$, for uncorrelated quenched noise and by spatio-temporal correlations, see also [14] for a different result. Recently, this study was extended to take into account the effects of different elastic interactions [15], from local to long range interactions, as well as possible dynamic effects such as elastic waves [8]. The extending in-plane tensile crack problem can be regarded as a specific example of driven elastic manifolds in random media [16–18].

Indeed this problem bare some strong similarities with other interface problems in condensed matter such as the dynamics of the solid–liquid–vapor contact line depinning for partially wetting liquid on a disordered substrate [19,20]. In the latter, the wandering exponent can be derived for weak disorder from scaling arguments [21,22], further developed in [20,23]. From these analysis, the wandering exponent for the lateral fluctuations of the contact line should be $\zeta \approx 1/2$ on length scales less than the Larkin length and $\zeta \approx 1/3$ on length scales between the Larkin and the capillary length. A functional renormalization calculation has been performed [24] for a field theoretical description of the dynamics of the contact line, subject to a uniform pulling force, using the formalism developed in [25,26]. The predicted wandering exponent was also $\zeta = 1/3$. Using the replica method, together with a Gaussian variational approximation, with replica symmetry breaking [28], it has been possible [27] to confirm the existence of the two scaling exponents already suggested [20,23] and to provide a quantitative computation of the correlation function of the contact line.

The aim of this paper is to go beyond our previous analysis of the dynamics of slow in-plane tensile crack along a disordered interface and to shed some light on the influence of possible correlations in the pinning forces, i.e. quenched heterogeneities, on the dynamics. This will be discussed with reference to recent experimental estimation of the scaling exponent. The paper is organized as follow: we introduce in Section 2 the experimental data and in Section 3, the model; in Section 4, we summarize the main results for uncorrelated uniform quenched disorder; in Sections 5 and 6, we present numerical predictions for the scaling of the correlation function of the crack front for short and long range correlated disorder along the interface; finally in Section 7 we point out some possible extensions of our study based on the comparison with experimental data.

2. Experiment

There has been very few experimental studies of the propagation of a single crack front along an interface (see e.g. Ref. [29] for an in-plane experiment in a slightly different context). Recently, Schmittbuhl and Måløy [30] provided an experimental study of the dynamics of a planar crack front along the annealed interface between two Plexiglas blocks. This interface was roughened, before the annealing, by sand blasting with grains of size $\approx 50 \mu\text{m}$. The size of the induced geometrical flaws on the interface can be measured experimentally and shown to scale with the grain size. The blocks are annealed together in a press at 205°C and then cooled down slowly. Roughness fluctuations of the interface induce, at the end of the annealing procedure, toughness variations along the interface. However, the details of the induced toughness disorder, such as the correlation length, is difficult to measure and have not yet been fully characterized even though it plays as we shall see an important role. A step by step loading with an imposed crack opening allows a very slow extension of the in-plane tensile crack. Typical velocities are within the range of 10^{-7}ms^{-1} to 10^{-5}ms^{-1} and the wandering exponent of the crack front is shown to be independent of the mean crack front velocity. All the experiments were made at room temperature. Direct observation of the crack-front geometry is possible due to the Plexiglas transparency. A microscope mounted on a translation stage equipped with a high resolution photographic camera (1536×1024 pixels) provides an accurate description of the crack front geometry and its evolution during the crack extension.

The correlation function of the position of the crack front is measured and shown to increase as a power law, which defines the wandering exponent ζ . The experimental prediction of the wandering exponent is found to be $\zeta \approx 0.55 \pm 0.05$. This experiment has been recently re-explored by Delaplace et al. [39] with a much higher resolution owing to the assembly of up to 12 pictures and a careful optical check of the set-up. The measured wandering exponent was found to be $\zeta = 0.63 \pm 0.03$. Both results agree within the error bars and are above the numerical prediction of $\zeta \approx 1/3$ [13].

3. The model

We consider here a half-plane tensile crack propagating through an unbounded elastic solid. The crack is restricted to move in the plane $x_3 = 0$, along the x_1 direction. The crack front position, at time t , is described by a curve $x_1 = \Phi(x_2, t)$ that is assumed to be single valued excluding configurations with overhangs. To first-order, $\Phi(x_2, t) = v_{cr}t + \phi(x_2, t)$ where v_{cr} is a uniform crack extension velocity and $\phi(x_2, t)$ are small amplitude distortions around that configuration with zero mean.

The energy per unit area of the interface that must be provided to fracture the solid is denoted $\Gamma(x_1 = \Phi(x_2, t), x_2)$. Interface heterogeneities are considered here as fluctuations in the local energy density: $\Gamma(x_1, x_2) = \Gamma_0[1 + \gamma(x_1, x_2)]$ where Γ_0 is the mean value of the interface toughness and $\gamma(x_1, x_2)$ random quenched fluctuations of zero mean.

The analysis is restricted to a scalar approximation of elasticity [5]. The displacement field is then a scalar variable $u(x_1, x_2, x_3, t)$ and the associated tensile stress across planes parallel to the crack is $\sigma = \mu \partial_{x_3} u$, with μ the elastic modulus. The problem is to find u satisfying the three-dimensional scalar wave equation: $c^2 \nabla^2 u = \partial^2 u / \partial t^2$ with the sound speed $c^2 = \mu / \rho$ where ρ is the density. The displacement field has a discontinuity across the crack surface $\Delta u(x_1, x_2, t) = u(x_1, x_2, 0^+, t) - u(x_1, x_2, 0^-, t)$, $\forall x_1 < \Phi(x_2, t)$. The stress must satisfy the boundary condition $\sigma = 0$ on the crack surface, i.e. $\partial_{x_3} u(x_1, x_2, x_3 = 0^\pm, t) = 0$ and meets the remote loading condition, i.e. the static external load. When the crack front arc has a continuously turning tangent, the structure of the singular field along a 3D crack edge is shown [5] to be the same as for solutions of the 2D plane strain, or anti-plane strain, crack extension problem at uniform (possibly zero) speed V_{cr} , where $u = u(x_1 - v_{cr}, x_2)$, and which has been extensively studied by Kostrov [31,32] and Eshelby [33]. Thus the stress field σ at distance $r = |\Phi(x_2, t) - x_1|$ ahead of the crack tip, on the plane $x_3 = 0$, has the square-root singularity $\sigma \propto (2\pi r)^{-1/2} K^\sigma(v)$ and the displacement discontinuity at distances r behind the crack tip satisfies $\Delta u \propto (r/2\pi)^{+1/2} K^u(v) / 2\mu$, where $K^\sigma(v) = K_{stat}(1 - v/c)^{1/2}$ and $K^u(v) = K_{stat}(1 + v/c)^{-1/2}$ are respectively the stress and strain dynamic intensity factors, with v the local propagation speed of the crack front, $v = \partial_t \Phi(x_2, t)$ and $v < c$.

The fracture energy G that is provided to the crack front by the flux of stored elastic energy per unit of new crack area can be written in terms of the stress and strain intensity factors $G(v) = K^\sigma(v)K^u(v) / 2\mu$ and has the general form [8]: $G(v) = f[v_\perp(x_2, t)]G_R$ where $v_\perp = \partial \Phi(x_2, t) / \partial t [1 + (\partial \Phi(x_2, t) / \partial x_2)^2]^{-1/2}$ is the local velocity normal to the crack front. The local rest value of the energy release rate G_R is then independent of v and depends of the prior growth history. When the crack front line is straight, and only outgoing waves are involved without effect of reflections from the opposite end of the crack, G_R has a simple form $G_R = G^\infty = K^{\infty 2} / 2\mu$ where K^∞ is the static remote load. The function $f(v_\perp)$ controls the fraction of the energy release rate available, it satisfies $f(0^+) = 1$ and $f(v_\perp) = 0$ when $v_\perp \rightarrow c$.

For small crack-front distortions, the energy release rate can be expanded about a uniformly extending crack [5,7,8], and to first-order:

$$G(v) = G_0(v_{\text{cr}}) \left[1 - \frac{1}{c\alpha^2(v_{\text{cr}})} \frac{\partial \phi(x_2, t)}{\partial t} + \mathcal{H}(x_2, t) \right], \quad (1)$$

where $\alpha(v_{\text{cr}}) = (1 - v_{\text{cr}}^2/c^2)^{1/2}$ and $G_0(v_{\text{cr}}) = ([1 - v_{\text{cr}}/c]/[1 + v_{\text{cr}}/c])^{1/2} G^\infty$. The nonlocal term is given by

$$\mathcal{H}(x_2, t) = \frac{1}{\pi} \int_{-\infty}^{\infty} \int_0^{\tau_m} \frac{c(t-t')[\partial_{t'} \phi(x'_2, t') - \partial_{t'} \phi(x_2, t)]}{(x_2 - x'_2)^2 [c^2 \alpha^2(v_{\text{cr}})(t-t')^2 - (x_2 - x'_2)^2]^{1/2}} dx'_2 dt' \quad (2)$$

with $\tau_m = \max\{0, t - |x_2 - x'_2|/\alpha(v_{\text{cr}})c\}$. If the equation of motion is supposed to be ruled by a local energy conservation, i.e. the local energy release rate criterion, we get

$$\frac{1}{c\alpha^2(v_{\text{cr}})} \frac{\partial \phi(x_2, t)}{\partial t} = \mathcal{H}(x_2, t) - \tau(x_1 = \Phi(x_2, t), x_2), \quad (3)$$

where the last term is the actual random driving force on the crack front line

$$\begin{aligned} \tau(x_1 = \Phi(x_2, t), x_2) &= \frac{\Gamma(x_1 = \Phi(x_2, t), x_2)}{G_0(v_{\text{cr}})} - 1 \\ &= \frac{\Gamma_0}{G_0(v_{\text{cr}})} [1 + \gamma(x_1 = \Phi(x_2, t), x_2)] - 1. \end{aligned} \quad (4)$$

With reference to the experimental conditions, discussed in the previous section, we make several simplifications. First, the averaged speed of the crack front is supposed to be slow, i.e. $v_{\text{cr}} \ll c$, thus $G_0(v_{\text{cr}}) \approx G^\infty$. Second, we assume that inertia is negligible, i.e. the dynamics is purely dissipative. The actual dynamics is therefore replaced by the adiabatic approximation, i.e. at each instant t of the evolution forces at every points balance exactly:

$$\mathcal{H}(x_2) - \tau(x_1 = \Phi(x_2), x_2) = 0, \quad (5)$$

where the nonlocal kernel is given by

$$\mathcal{H}(x_2) = \frac{1}{\pi} \int_{-\infty}^{\infty} \frac{\phi(x'_2) - \phi(x_2)}{(x_2 - x'_2)^2} dx'_2. \quad (6)$$

The final Hamiltonian for the quasi-static evolution of the crack front line is thus given by

$$\begin{aligned} H &= \frac{1}{2} \int_k |k| |\phi(k)|^2 dk + \int_0^L V(\Phi(x_2), x_2) dx_2, \\ V(\Phi(x_2), x_2) &= \int_0^{\Phi(x_2)} \tau(x_1, x_2) dx_1, \end{aligned} \quad (7)$$

where $V(\Phi(x_2), x_2)$ is a random potential.

We shall consider in the following a periodic in-plane crack front in x_2 , with a spatial period L and slow a propagation speed $v/c \ll 1$. This requires a summation

of the nonlocal kernel over all the periods and modifies the $1/x^2$ interaction to be $(\pi/L)^2/\sin^2(\pi x/L)$. The nonlocal kernel becomes therefore, at any time t

$$\mathcal{H}(x_2) = \frac{\pi}{L^2} \int_0^L \frac{\phi(x'_2) - \phi(x_2)}{\sin^2[\frac{\pi}{L}(x'_2 - x_2)]} dx'_2. \tag{8}$$

The model is then discretized for numerical simulations. In the x_2 direction, the crack front line is described as a periodic array of sites. The unit length along the x_2 direction is given by the distance between the sites and therefore the system size is L with L -nodes. In all the computations we make use of large system size $L = 4096$. Since we are interested in the case of very slow extension of the in-plane crack, extremal dynamics (ED) is very appealing because it allows to grasp the many metastable configurations of the problem. Extremal dynamics is based on the assumption that only one site of the crack front line is allowed to evolve during one time step, i.e. at each step the system is loaded by tuning G_0 in order to bring the most susceptible site along the crack front up to instability:

$$G_0 = \Gamma_0 \min_{x_2} \left\{ \frac{1 + \gamma(x_1, x_2)}{1 + \mathcal{H}(x_2)} \right\}. \tag{9}$$

This search defines also the position of the most susceptible site on the crack front. The local dynamics is not solved exactly and the crack front line is depinned at this site with a jump of a fixed amount δx that gives the unit length in the direction of propagation. The local random driving force is locally updated according to the adopted random distribution. At that stage, the crack is unloaded and all the forces along the crack front line are modified according to the discretized non-local kernel. The procedure is then repeated. The time scale is fixed by the frequency of the updates of single sites and not directly related to the real time measured in experiment. All the simulations start with a flat uniform crack front and run over a long sequence of such steps, more than 10^6 , after the initial transient.

Starting with a straight crack front line, the system organizes after a transient regime into a statistically highly correlated stationary state. Experimentally the correlation function of the position of the crack front line in the x_2 direction $\langle (\Phi(x_2) - \Phi(x'_2))^2 \rangle = \langle (\phi(x_2) - \phi(x'_2))^2 \rangle$ can be computed. One manifestation of these long range correlations is the roughening of the crack front line that is characterized by the scaling of the correlation function that increases as a power law, and defines locally the wandering exponent ζ

$$\langle (\phi(x_2) - \phi(x'_2))^2 \rangle \propto |x_2 - x'_2|^{2\zeta}. \tag{10}$$

The power-law behavior of the correlation function have been analyzed using several methods: variable bandwidth, return probability, Fourier spectrum [34] and the recently proposed wavelet analysis [36]. The results are shown here using the latter technique. Averaging out the dependency on the translation parameter, the wavelet transform of the crack-front line is shown to obey:

$$\mathcal{W}[\phi](\lambda a) = \langle \mathcal{W}[\phi](\lambda a, \lambda b) \rangle_b \propto \lambda^{\frac{1}{2} + \zeta} \mathcal{W}[\phi](a), \tag{11}$$

where $\mathcal{W}[\phi](a, b)$ is the wavelet transform of the crack-front line perturbation and (a, b) the dilatation and translation parameters of the analyzing wavelet.

4. Uniform quenched disorder

We shall suppose that the fluctuations, $\Gamma_0\gamma$, of the local toughness, i.e. the pinning energy per unit area, are quenched and are described by a flat distribution. This leads to a random force problem that was analyzed in details [13,15]. We just recall here the main results of these studies.

The power-law behavior of the correlation function of the position of the crack front in the statistically stationary state, using the wavelet analysis, are shown on Fig. 1b. The wandering exponent ζ is found to be $\zeta \approx 0.35 \pm 0.02$ that is consistent with previous studies [13,15].

The roughness over a local length scale l , $W(l, t) = \langle [\Phi(x_2, t) - \langle \Phi \rangle(t)]^2 \rangle_{x_2}^{1/2}$ evolves with time during a transient regime. We checked that, in the case of large fluctuation regimes, such an evolution follows a Family–Viscek scaling. The wavelet transform of the crack-front profile scales therefore as:

$$\mathcal{W}[\phi(\cdot, t)](a) = a^{\zeta + \frac{1}{2}} g\left(\frac{a}{t^{1/2}}\right), \quad (12)$$

where ζ and z are the wandering and the dynamic exponents. The scaling function behaves as $g(u) = 1$ if $u \ll 1$, and $g(u) \propto u^{-\zeta - 1/2}$ if $u \gg 1$. The dynamic exponent controls the time evolution of the roughness during the transient regime. The local roughness saturates at time t^z as $W(l, t \gg t^z) \propto l^\zeta$ independently of the system size and therefore is statistically self-affine up to a correlation length ξ that grows with time as $\xi \propto t^{1/2}$. We find, Fig. 1a, a dynamic exponent $z \approx 0.75$ in close agreement with our previous study [13] and the functional renormalization group analysis [24,35].

The active sites, in the statistically stationary state ($t \gg L^z$), were shown to be spatially and temporally correlated [13,15]. In order to analyze these correlations, it is of interest to study the probability distribution $p(|x_2 - x'_2|, \Delta t)$ of having a distance $|x_2 - x'_2|$ between the sites active at time t and $t + \Delta t$ [37]. From the numerical simulations, it is possible to estimate the distribution as

$$p(|x_2 - x'_2|, \Delta t) = \Delta t^{1/\beta} g\left(\frac{|x_2 - x'_2|}{\Delta t^{1/\beta}}\right) \quad (13)$$

with a dynamic exponent β that describe the spreading of the activity over a zone of size $\xi \propto \Delta t^{1/\beta}$. The scaling function g behaves as $g(u) \propto u^a$ for $u \ll 1$ and $g(u) \propto u^{-b}$ for $u \gg 1$. The numerical results, Fig. 2, show a data collapse for $a = 0$, $b \approx 1.9$ and $\beta \approx 1.33$, that is in close agreement with the result of [15]. It is possible in this case to link the exponent β to the wandering exponent using a simple scaling argument. Since the average time for the spreading of the activity is $\tau(\xi) \propto \xi^\beta$ and the number of depinned sites to cover this area after a time Δt is $\propto \xi \delta x \propto \xi^{1+\zeta}$, we get $\beta = 1 + \zeta$. If we consider two consecutive events, the probability distribution decays as a power

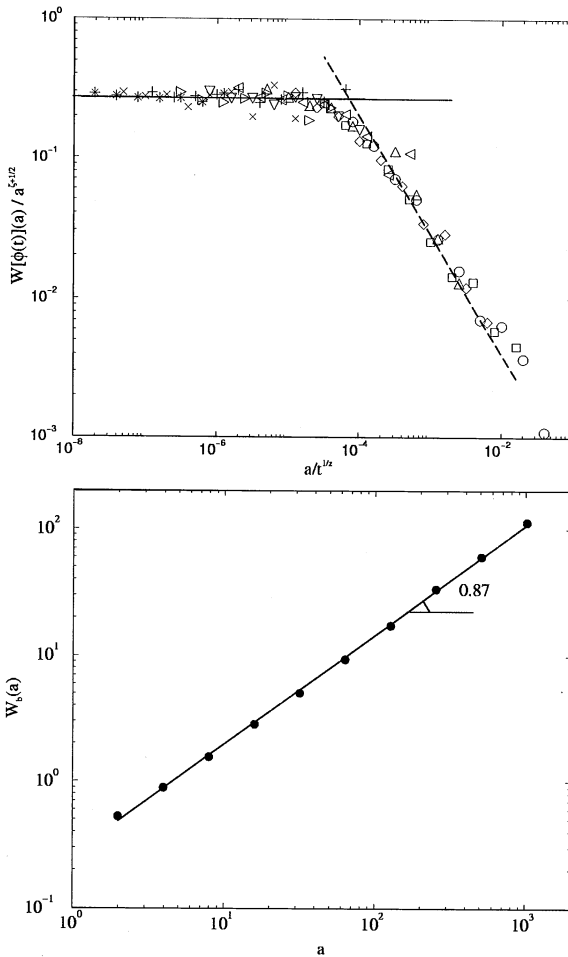


Fig. 1. Scaling of the crack-front line for uniform quenched disorder. (a) Family–Viscek scaling in the transient using average wavelet analysis. Symbols correspond to a different time steps (using a geometry serie). The power law fit corresponds to $\zeta = 0.35$ and the collapse is obtained for $z = 0.75$. (b) Scaling of the correlation function in the statistically stationary state using average wavelet transform. The straight line shows a power-law fit that corresponds to $\zeta = 0.37$.

law $p(|x_2 - x'_2|, 1) \propto |x_2 - x'_2|^{-b}$ and is controlled by the singularity of the non-local elastic kernel. On the other hand, the probability of having a recurrent event at the same location on the crack-front line $p(1, \Delta \rightarrow \infty)$ is high and does not evolve with time, since $a = 0$. This is consistent with the observed clustering in space.

5. Quenched disorder with short-range correlations

We shall suppose now that the fluctuations, $\Gamma_0\gamma$, of the local toughness, results from a large number of small scale interactions and obey Gaussian distributions with zero

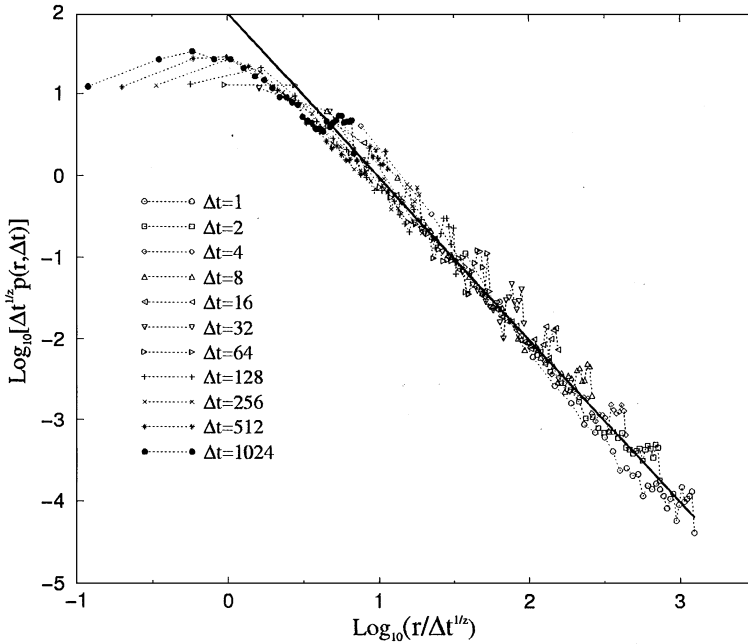


Fig. 2. Furuberg analysis of the spatio-temporal correlations in the stationary state for uniform quenched disorder. The power law fit corresponds to $b = 2.0$ and the best collapse is obtained for $\beta = 1.33$.

mean. These fluctuations are assumed to be spatially correlated on short range and describe by a Gaussian correlation function with a correlation length Δ : $\langle \tau(x_1, x_2) \tau(x'_1, x'_2) \rangle = v \langle \gamma(x_1, x_2) - \gamma(x'_1, x'_2) \rangle = v \Upsilon(x_1 - x'_1, x_2 - x'_2)$ where $v = \Gamma_0/G_0$ and Υ is a function that decays rapidly for large values of its argument. In most physical situations, the distribution of disorder can be assumed to be isotropic in the $x_1 - x_2$ plane. However, the correlation in the x_2 direction has only small effects on very short distances, the coarse-graining length, and is not relevant experimentally. The pair correlation function is thus assumed to be asymmetric [27]

$$\Upsilon(x_1 - x'_1, x_2 - x'_2) = \frac{W}{\Delta^2} \delta(x_2 - x'_2) C \left(\left| \frac{x_1 - x'_1}{\Delta} \right| \right), \quad (14)$$

where the correlation function satisfies $C(0) = 1$, $C''(0) = -1$, with $C(r) \approx 0$ for $|r| \gg 1$, and is assumed for simplicity to be $C(r) = e^{-r^2/2}$. The random potential term $V(\Phi(x_2), x_2)$, as the sum of independent Gaussian variables, is Gaussian distributed [27] and, for the specific choice of the correlation function C , given by

$$\langle V(\Phi, x_2) V(\Phi', x'_2) \rangle = -W \delta(x_2 - x'_2) f \left(\left[\frac{\Phi - \Phi'}{\Delta} \right]^2 \right), \quad (15)$$

where

$$f(u^2) = |u| \int_0^{|u|} e^{-v^2/2} dv - (1 - e^{-u^2/2}). \quad (16)$$

5.1. Roughness in the regime of small fluctuations

We first consider the regime where the fluctuations of the crack front line is small compared with the correlation length Δ , i.e. $|\phi(x_2) - \phi(x'_2)| \ll \Delta$. In this case, the potential term can be linearized and to first order

$$V(\Phi(x_2), x_2) \simeq V(\langle \Phi \rangle, x_2) - v\tau(\langle \Phi \rangle, x_2)\phi(x_2) \tag{17}$$

with a force correlation function $v\langle \gamma(\langle \Phi \rangle, x_2)\gamma(\langle \Phi \rangle, x'_2) \rangle = v\frac{W}{\Delta^2}\delta(x_2, x'_2)$. The Hamiltonian can be rewritten as [27]

$$H = \frac{1}{2} \int_k \left| k \left| \phi(k) - \frac{\gamma(k)}{v|k|} \right| \right|^2 dk - \frac{1}{v^2} \int_k \frac{|\gamma(k)|^2}{|k|} dk \tag{18}$$

and therefore at large separations $|x_2 - x'_2| \gg \Delta$,

$$\langle (\phi(x_2) - \phi(x'_2))^2 \rangle = \frac{W}{v^2 \Delta^2} \int_k \frac{2 - 2 \cos(k(x_2 - x'_2))}{k^2} dk = \frac{W}{v^2 \Delta^2} |x_2 - x'_2|. \tag{19}$$

The predicted exponent in this regime, i.e. the Larkin regime, is thus given by $\zeta = 1/2$ for $|x_2 - x'_2| \ll \xi$, where ξ is the Larkin length, $\xi = v^2 \Delta^2 / W$.

The crack-front line evolution and the power-law behavior of the correlation function in the statistically stationary state, using a wavelet analysis, are shown on Fig. 3. In order to resolve this regime, the parameters of the numerical simulation have been set to $W = 10^{-2}$, $\Delta = 3$ and $\delta x = 10^{-2}$. At small length scales, we determine a wandering exponent $\zeta = 0.50 \pm 0.02$ in good agreement with the perturbation theory prediction and the analytic replica method [27].

5.2. Roughness in the regime of large fluctuations

On larger length scales, $|x_2 - x'_2| > \xi$, the fluctuations of the line are greater than the correlation length Δ , $|\phi(x_2) - \phi(x'_2)| > \Delta$, and the potential term in the Hamiltonian can no longer be linearized. One can then estimate the wandering exponent by a simple scaling argument of Mézard and Parisi [28,27]. The scale transformation $x_2 \rightarrow lx_2$, $\Phi(x_2) \rightarrow l^\zeta \Phi(x_2)$, $V(\Phi(x_2), x_2) \rightarrow l^\lambda V(\Phi(x_2), x_2)$, imposing that the two terms in the Hamiltonian scale the same way and that the potential term keeps the same statistics after rescaling, leads $\lambda = 2\zeta - 1$ and $2\lambda = -1 + \zeta$ and so $\zeta = 1/3$ which is less than the value obtained in the Larkin regime and coincides with our result for the uncorrelated quenched uniform disorder case. This value of the wandering exponent can also be recovered by the Imry–Ma estimate of Huse given in [20]. It also consistent with the renormalization group analysis using the formalism developed in [25,26] and, more recently, the analytical results obtained using the replica method approach [27].

This regime can be numerically study for a fixed system size L by assigning a very low value to Δ . Due to discreteness of the numerical model, assigning a small value Δ , compared to the grid size, is the same as considering a uniform random distribution for the driving force $\tau(x_1, x_2)$ and all the previous scaling, for uniform quenched disorder, can be recovered.

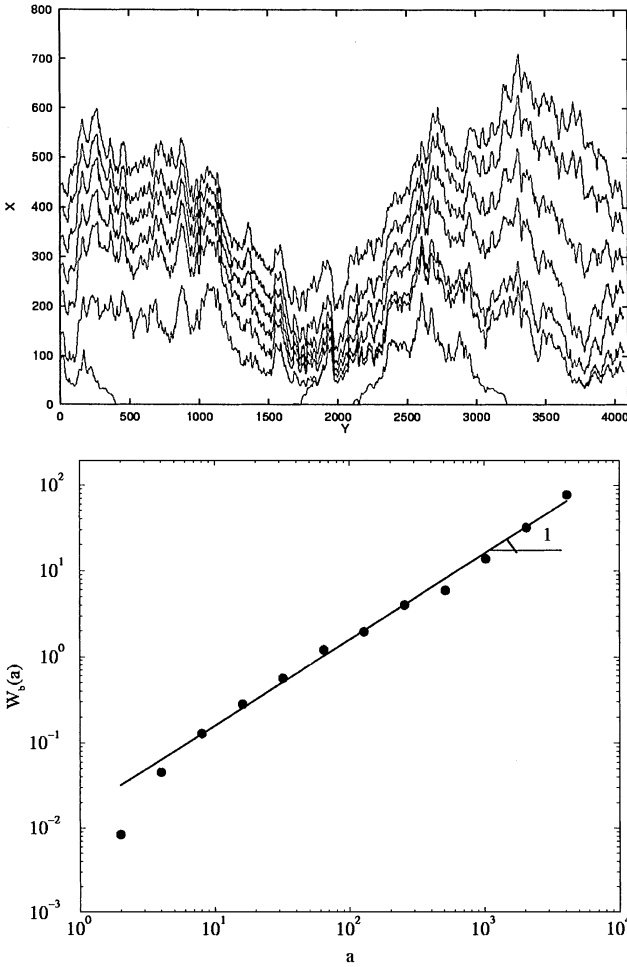


Fig. 3. Roughness of the crack-front line in the statistically stationary state for small fluctuations: top, crack front line geometry at different time intervals; bottom, average wavelet transform of the displacement crack-front position. The straight line shows a power-law fit that corresponds to $\zeta = 0.50$. The lower cut-off corresponds to length scales $|x_2 - x'_2| \approx \Delta$.

6. Quenched disorder with long-range correlations

We consider here the case where the fluctuations, $\Gamma_0 \gamma$, of the local toughness are Gaussian with zero mean and are spatially correlated with long range correlations, i.e. the toughness correlations are controlled by a self-affine exponent ζ_t . In this case the correlation function Υ has now a slow algebraic decay. The random force correlation function is assumed to behave as

$$\Upsilon(x_1 - x'_1, x_2 - x'_2) \propto |(x_1 - x'_1)^2 + (x_2 - x'_2)^2|^{\zeta_t} \quad (20)$$

and in Fourier space $\Upsilon(\mathbf{k}) \propto k^{2-2\zeta_t}$.

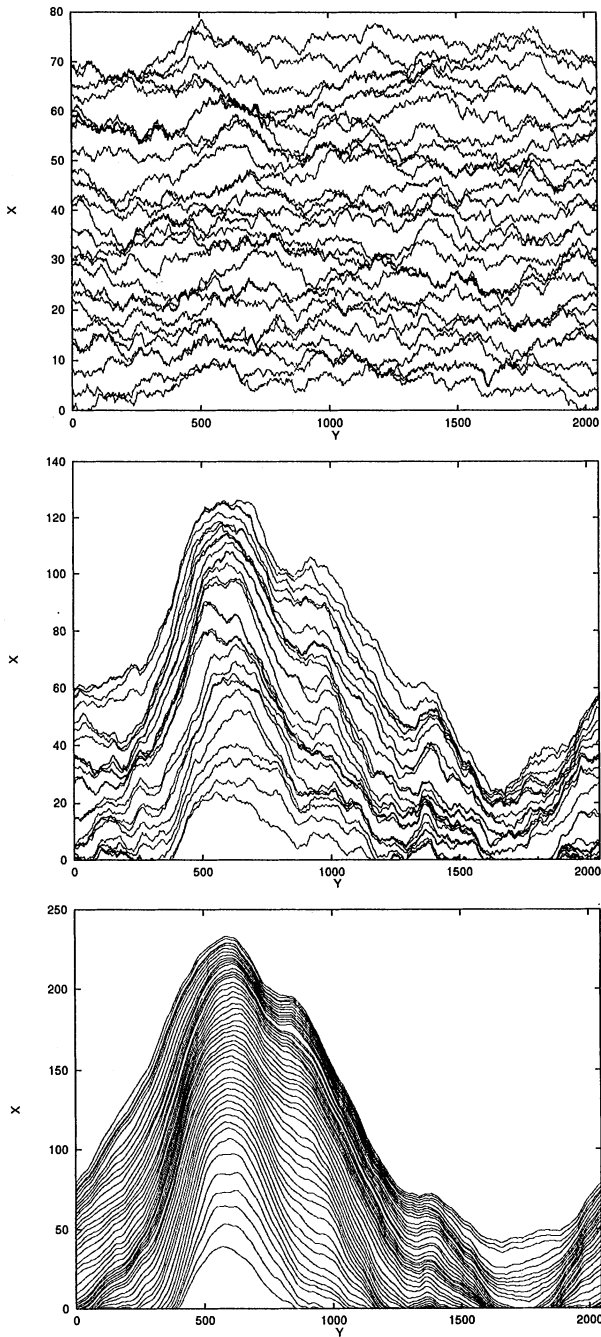


Fig. 4. Crack-front line profile in the case of long range correlations. The quenched disorder correlations are controlled by a self-affine exponent ζ_l : from top to bottom: $\zeta_l = -0.5$, $\zeta_l = 0$, $\zeta_l = 0.5$.

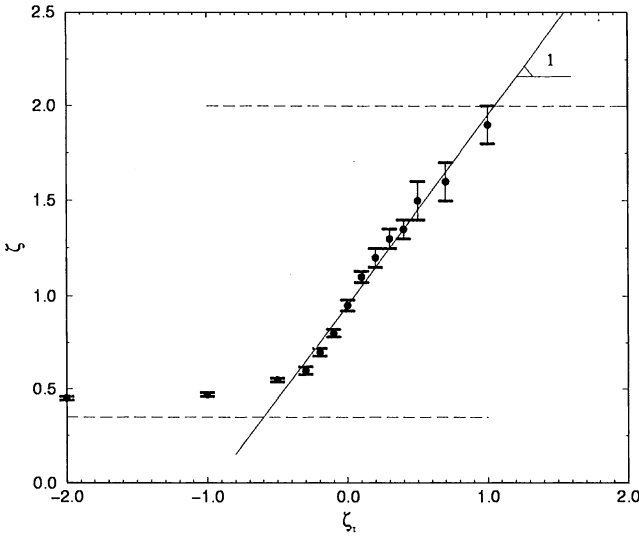


Fig. 5. Wandering exponent ζ of the crack-front line correlation function as a function of the self-affine exponent of the long range correlated quenched disorder ζ_t .

Several algorithms exist for the generation of such self-affine surfaces. We used in this study the Voss algorithm [38] and the Fourier transform. The latter make use of the scaling property of the Fourier spectrum. In the Fourier space, one generate a surface $\tau(\mathbf{k})$ with a module that follows the scaling $|\tau(\mathbf{k})| \propto |k|^{-2-\zeta_t}$ with a random phase. The conditions $\tau(-\mathbf{k}) = -\tau(\mathbf{k})$ insures a nil imaginary part after the inverse transform.

The case of long range correlations in the quenched disorder has not yet been studied using the functional group analysis. Numerically, the evolution of the crack-front line geometry, in the statistically stationary regime, is shown on Fig. 4 and the evolution of the wandering exponent of the crack front line correlations as a function of the self-affine exponent of the quenched disorder correlations is shown on Fig. 5.

As the exponent ζ_t increases, small scale fluctuations decreases and the crack-front line becomes smoother and smoother. For small values of ζ_t , the crack-front line geometry is closed to the one obtained in the case of uniform random disorder. The elastic interactions are shown to significantly increase any long range disorder correlations in the system. For $\zeta_t > -1.0$, small scale correlations decrease and one can approximate the quasi-static evolution as

$$|k|\phi(k) \approx -v\gamma(\langle\Phi\rangle, k) \quad (21)$$

That would lead to a scaling, to first order in small scale correlations

$$\langle|\phi(k)|^2\rangle \propto \frac{\Upsilon(\mathbf{k})}{|k|^2} \propto |k|^{-2-2(\zeta_t+1)} \quad (22)$$

which is effectively observed numerically up to $\zeta_t \approx 1$.

7. Conclusions

We have studied the slow dynamics of in-plane crack propagation including the effects of long range elasticity and those of spatial correlations in the toughness of the interface. Quenched noise correlations are shown to influence significantly the development of the crack-front line correlations during in-plane crack propagation at low speed. In the case of short-range Gaussian correlations, with correlation length Δ , two limit behaviors can be identified. In the small fluctuations limit, $|\phi(x_2) - \phi(x'_2)| \ll \Delta$, on length scales smaller than the Larkin length, the wandering exponent of the crack-front line is $\zeta/2$. For large fluctuations, $|\phi(x_2) - \phi(x'_2)| \gg \Delta$, on length scales larger than the Larkin length, the wandering exponent is smaller with $\zeta/3$. The latter is in good agreement with the wandering exponent prediction using functional renormalization group analysis [24] or the replica method [27]. The scaling in the large fluctuations limit is also in good agreement with previous numerical studies with a uniform quenched disorder. In the case of long-range correlations, for which no analytical results exist, the numerical study predict a strong amplification of the crack-front line correlations that scale directly as $\zeta_t + 1$, where ζ_t is the self-affine exponent that describes the long range correlations of the quenched disorder.

Recent experimental studies [30,39] of in-plane crack propagation between two annealed blocks of Plexiglas suggest a wandering exponent of the crack-front line $\zeta = 0.63 \pm 0.03$. This is higher than the value obtained for a uniform quenched disorder in the interface toughness and for the large fluctuations regime in case of short-range Gaussian correlations. The crack speed in the experiment is very low and the fluctuations of the crack-front line position remain small. This seems to be closer to the small fluctuations regime of short-range Gaussian correlations. In this regime the predicted wandering exponent is closer to the experimental one but still underestimate the experimental value. In case of long-range fluctuations, the experimental wandering exponent may be recovered when assuming toughness long-range correlations with a self-affine exponent of $\zeta_t \approx -0.4$. However, it is difficult to analyze experimentally the toughness fluctuations induced by the experiment set-up and such an analysis has not yet been done. Other explanation for this experimental value has been proposed. The first one [35] is that the experiments are not quasi-static and even though the averaged crack speed remains slow, crack front wave instabilities may enhance the crack-front line correlations. An other possibility, is that at slow speed viscoelastic effects may operate.

Acknowledgements

The present text benefited from discussions with Stéphane Roux, Anne Tanguy, Arnaud Delaplace and Knut Jørgen Måløy.

References

- [1] H. Gao, J.R. Rice, *J. Appl. Mech.* 53 (1986) 774.
- [2] H. Gao, J.R. Rice, *J. Appl. Mech.* 56 (1989) 828.

- [3] H.F. Bueckner, *Zeit. Angew. Math. Mech.* 50 (1970) 529.
- [4] J.R. Rice, *J. Appl. Mech.* 52 (1985) 571.
- [5] J.R. Rice, Y. Ben-Zion, K. Kim, *J. Mech. Phys. Solids* 42 (1984) 813.
- [6] G. Perrin, J.R. Rice, *J. Mech. Phys. Solids* 42 (1994) 1047.
- [7] J.R. Willis, A.B. Movchan, *J. Mech. Phys. Solids* 43 (1995) 319.
- [8] S. Ramanathan, D.S. Fisher, *Phys. Rev. Lett.* 79 (1997) 877.
- [9] H. Gao, *J. Appl. Mech.* 59 (1992) 335.
- [10] G. Xu, A.F. Bower, M. Ortiz, *Int. J. Solids Struct.* 31 (1994) 2167.
- [11] S. Ramanathan, D. Ertaz, D.S. Fisher, *Phys. Rev. Lett.* 79 (1987) 873.
- [12] J.R. Willis, A.B. Movchan, *J. Mech. Phys. Solids* 45 (1997) 591.
- [13] J. Schmittbuhl, S. Roux, J.P. Vilotte, K.J. Måløy, *Phys. Rev. Lett.* 74 (1985) 1787.
- [14] P.B. Thomas, M. Paczuski, *cond-mat* 9602023.
- [15] A. Tanguy, M. Gounelle, S. Roux, *Phys. Rev. E* 58 (1998) 1577.
- [16] T. Halpin-Healy, Y.C. Zhang, *Phys. Rep.* 254 (1995) 215.
- [17] H. Leschborn, T. Nattermann, S. Stepanow, L.H. Tang, *cond-mat* 9603114.
- [18] D.S. Fisher, *cond-mat* 9711179.
- [19] J.F. Joanny, P.G. de Gennes, *J. Chem. Phys.* 81 (1984) 552.
- [20] P.G. de Gennes, *Rev. Mod. Phys.* 57 (3) (1985) 827.
- [21] A.I. Larkin, *Sov. Phys. JETP* 31 (1970) 784.
- [22] Y. Pomeau, J. Vannimenus, *J. Colloid Interface Sci.* 104 (1985).
- [23] M.O. Robbins, J.F. Joanny, *Europhys. Lett.* 3 (1987) 729.
- [24] D. Ertaz, M. Kardar, *Phys. Rev. E* 49 (1994).
- [25] P.C. Martin, E. Siggia, H. Rose, *Phys. Rev. A* 8 (1973) 423.
- [26] O. Narayan, D.S. Fisher, *Phys. Rev. B* 48 (1993) 7030.
- [27] A. Hazareesing, M. Mézard, *cond-mat* 9806373.
- [28] M. Mézard, G. Parisi, *J. Phys. (France) I* 1 (1991) 809.
- [29] T. Mower, A.S. Argon, *Mech. Mat.* 19 (1995) 343.
- [30] J. Schmittbuhl, K.J. Måløy, *Phys. Rev. Lett.* 78 (1997) 3888.
- [31] B.V. Kostrov, *Appl. Math. Mech.* 30 (1966) 1241 (English translation of *Prikl. Mat. i Mech.*).
- [32] B.V. Kostrov, *Int. J. Fract.* 11 (1975) 47.
- [33] J.D. Eshelby, *J. Mech. Phys. Solids* 17 (1969) 177.
- [34] J. Schmittbuhl, J.P. Vilotte, S. Roux, *Phys. Rev. E* 51 (1995) 131.
- [35] S. Ramanathan, D.S. Fisher, *cond-mat* 9712181.
- [36] I. Simosen, A. Hansen, O. Magnar Ness, *Phys. Rev. E* 58 (1998) 2779.
- [37] L. Furuberg, J. Feder, A. Aharony, T. Jossang, *Phys. Rev. Lett.* 61 (1998) 2117.
- [38] R.F. Voss, in: R.A. Earnshaw (Ed.), *Fundamentals Algorithms in Computer Graphics*, Springer, New York, 1985.
- [39] A. Delaplace, J. Schmittbuhl, K.J. Måløy, *Phys. Rev. E*, in press.